Published in final edited form as:
Genes Dev. 2001 June 1; 15(11): 1427–1434.

A mutation in the Gsk3–binding domain of zebrafish Masterblind/Axin1 leads to a fate transformation of telencephalon and eyes to diencephalon

Carl-Philipp Heisenberg[1,5], **Corinne Houart**[1,6], **Masaya Takeuchi**[1,6], **Gerd-Jörg Rauch**[2], **Neville Young**[3], **Pedro Coutinho**[4], **Ichiro Masai**[1], **Luca Caneparo**[1], **Miguel L. Concha**[1], **Robert Geisler**[2], **Trevor C. Dale**[3], **Stephen W. Wilson**[1,7], and **Derek L. Stemple**[4]

1*Department of Anatomy and Developmental Biology, University College London, London WC1E 6BT, UK;*

2*Abteilung Genetik, Max-Planck-Institut für Entwicklungsbiologie, 72076 Tübingen, Germany;*

3*Developmental Biology, Section of Cell Biology and Experimental Pathology, Toby Robins Breakthrough Breast Cancer Research Center, Institute of Cancer Research, London SW3 6JB, UK;*

4*Division of Developmental Biology, National Institute of Medical Research, Mill Hill, London NW7 1AA, UK*

Abstract

Zebrafish embryos homozygous for the *masterblind* (*mbl*) mutation exhibit a striking phenotype in which the eyes and telencephalon are reduced or absent and diencephalic fates expand to the front of the brain. Here we show that $mbl^{-/-}$ embryos carry an amino-acid change at a conserved site in the Wnt pathway scaffolding protein, Axin1. The amino-acid substitution present in the *mbl* allele abolishes the binding of Axin to Gsk3 and affects Tcf-dependent transcription. Therefore, Gsk3 activity may be decreased in $mbl^{-/-}$ embryos and in support of this possibility, overexpression of either wild-type Axin1 or Gsk3β can restore eye and telencephalic fates to $mbl^{-/-}$ embryos. Our data reveal a crucial role for Axin1-dependent inhibition of the Wnt pathway in the early regional subdivision of the anterior neural plate into telencephalic, diencephalic, and eye-forming territories.

Keywords

Axin; Wnt; forebrain; zebrafish

Although considerable progress has been made in elucidating the genetic pathways that regulate dorsoventral patterning of the vertebrate CNS (Lee and Jessell 1999;Jessell 2000), it remains uncertain how early anterior-posterior (AP) pattern is established (Lumsden and Krumlauf 1996). Studies performed mainly in amphibia have suggested various models of AP patterning in which early neural tissue has anterior character upon which posterior character is imposed by signals originating in more caudal regions of the embryo (Gamse and Sive 2000). Among the signals that are suggested to influence regional identity along the AP axis are Fgfs, retinoic acid, Nodals, and Wnt proteins (Gamse and Sive 2000;Wilson and Rubenstein 2000).

[7]**Corresponding author. E-MAIL** s.Wilson@ucl.ac.uk; FAX 207-679-7349.
Present address: Max-Planck-Institute for Molecular Cell Biology and Genetics, Pfotenhauerstr. 108, 01307 Dresden, Germany.
[6]These authors contributed equally to this work.

Misexpression studies have suggested that suppression of Wnt signaling is required for induction of the vertebrate head (Niehrs 1999). Direct genetic evidence supporting this conclusion has come from the recent demonstration that *headless* (*hdl*) mutant zebrafish embryos carry a mutation that abolishes the repressor function of Tcf3, a transcriptional modulator of Wnt signaling (Kim et al. 2000). Although the evidence implicating the Wnt pathway in head development is substantial, it remains to be determined where, when, and how Wnt signaling must be suppressed to promote head formation.

Levels of Wnt signaling can be regulated negatively through the activity of a variety of extracellular proteins that include members of the Cerberus, Dickkopf, and Sfrp families (Niehrs 1999). Additionally, several intracellular components of the Wnt signaling pathway can modulate the degree to which Wnt target genes are activated or repressed (Brown and Moon 1998;Wodarz and Nusse 1998). For instance, the protein kinase Gsk3 phosphorylates β-catenin, targeting it for degradation (Aberle et al. 1997;Ikeda et al. 1998;Kishida et al. 1999), thereby limiting the amount of β-catenin available to activate Wnt target genes. Gsk3 functions in multicomponent complexes, one of which appears to include adenomatous polyposis coli, Axin, and additional proteins (Kim et al. 1999;Barker and Clevers 2000). Within this complex, Axin is believed to function as a scaffolding protein that enables Gsk3 to efficiently colocalize with, and thereby phosphorylate β-catenin (Ikeda et al. 1998;Kishida et al. 1999). The eventual nuclear readout of Wnt signals therefore can be modulated in many ways and at several different positions in the Wnt signal transduction pathway.

In this study, we show that alterations in Wnt signaling underlie one of the most dramatic mutations known to affect AP patterning of the brain. *masterblind* (*mbl*) mutant embryos exhibit major fate switches within the prospective forebrain and here we show that the *mbl* phenotype is a result of a mutation in Axin1 that leads to overactivation of Wnt signaling.

Results and Discussion

mbl *mutant embryos show a fate transformation of telencephalon and eyes to diencephalon*

Zebrafish homozygous for the *mbl*^{tm213} mutation (*mbl*$^{-/-}$) possess a head but exhibit major alterations in fate allocation within the forebrain such that eyes and telencephalon are reduced or absent while the diencephalic epiphysis is expanded anteriorly (Heisenberg et al. 1996;Masai et al. 1997) (Fig. 1A–F). The expressivity of the *mbl*$^{-/-}$phenotype is temperature-dependent and small eyes are present in 20% of mutants reared at 22°C (Fig. 1C,D) while they are absent when rearing is at 30°C (Fig. 1E,F). This suggests that the *mbl* allele may generate a protein that has temperature-dependent activity.

The fate changes within the forebrain of *mbl*$^{-/-}$ embryos are reflected in alterations to the expression of genes within the anterior neural plate from gastrulation stages onwards. In *mbl*$^{-/-}$ embryos, genes expressed in the prospective telencephalon (*anf, emx1;* Fig. 1G–J) and eyes (*rx3;* Fig. 1K,L) are reduced or absent by bud stage, whereas genes expressed within the mid/caudal diencephalon (*fkd3*, *deltaB;* Fig. 1M–P) are expanded anteriorly. In contrast, the expression domains of genes within the prospective midbrain (*pax2.1*) are only mildly altered or show no obvious changes in *mbl*$^{-/-}$ embryos (Fig. 1Q,R). These results indicate that anterior forebrain territory adopts posterior forebrain character by late gastrulation in *mbl*$^{-/-}$ embryos.

mbl$^{-/-}$ *embryos carry a mutation in the Gks3 binding domain of Axin1*

To understand the role of Mbl in early forebrain patterning, we identified the mutation likely to be responsible for the *mbl*$^{-/-}$ phenotype. Mapping of the *mbl* mutation showed it to be adjacent to the centromeric region of linkage group 3, close to the Wnt scaffolding protein encoding gene, *axin1* (Shimizu et al. 2000) (Fig. 2A). Mice lacking Axin function have axis

duplications (Jacobs-Cohen et al. 1984), supporting the conclusion that Axin is a negative regulator of Wnt signaling (Zeng et al. 1997). As suppression of Wnt signaling can promote anterior fates (Niehrs 1999), we tested *axin1* as a candidate for harboring the *mbl* mutation. Sequencing of the *mbl axin1* allele revealed a leucine to glutamine (L→Q) amino-acid exchange at position 399 within the Gsk3 binding domain (Ikeda et al. 1998) of Axin1 (Fig. 2B) raising the possibility that altered Axin1 function indeed could be responsible for the $mbl^{-/-}$ phenotype.

To determine if *axin1* is expressed at appropriate times and places to regulate early forebrain patterning, we analysed *axin1* RNA distribution. *axin1* is maternally provided and ubiquitously expressed throughout early development with slightly higher expression anteriorly at the end of gastrulation (Fig. 2C–F). The expression of *axin1* is not noticeably changed in $mbl^{-/-}$ mutant embryos (data not shown). Axin1 therefore is likely to be present throughout the embryo at stages when we believe Mbl function is required.

To test if altered Axin1 function is indeed responsible for the $mbl^{-/-}$ phenotype, we provided $mbl^{-/-}$ embryos with RNA encoding wild-type Axin1. Widespread expression of wild-type *axin1* RNA in $mbl^{-/-}$ embryos efficiently rescues early neural plate patterning and restores eyes and telencephalic structures at later stages (Fig. 2G–L; Table 1). In contrast, injection of equivalent (or higher) levels of *mbl axin1* RNA into $mbl^{-/-}$ embryos did not rescue the $mbl^{-/-}$ phenotype (Table 1; data not shown). Therefore, the mutation within Axin1 is likely to be responsible for the fate transformations within the anterior neural plate of $mbl^{-/-}$ embryos.

Axin1/Gsk3 interactions are disrupted by the mbl *mutation*

The L→Q amino-acid change in Axin1/Mbl occurs within the Gsk3 binding domain (e.g., Ikeda et al. 1998) raising the possibility that Axin1/Gsk3 interactions may be disrupted in $mbl^{-/-}$ embryos. Mutations at the same or nearby sites in human Axin have been identified in cells from colon cancers and in vitro assays have shown that such mutations can reduce binding of Axin to Gsk3 (Webster et al. 2000). We therefore introduced the L→Q amino-acid change at an equivalent position in a murine Axin construct (Fig. 3A) and tested if this affects binding to Gsk3. Gsk3 is efficiently immunoprecipitated by the wild-type Axin construct but not by the Axin construct incorporating the *mbl* mutation (Fig. 3B). Therefore, the L→Q amino-acid exchange in *mbl* Axin1 is likely to impair Axin1 binding to Gsk3 in $mbl^{-/-}$ embryos.

Mutations in the Gsk3 binding site of murine Axin can lead to mutant forms of Axin functioning in a dominant negative way, most likely by interfering with wild-type Axin function (Smalley et al. 1999). Therefore, we examined if Axin constructs incorporating the L→Q amino-acid exchange show any dominant negative effects. Tcf-dependent transcription is increased in the presence of Axin1 constructs incorporating the L→Q amino-acid exchange while it shows little or no change in the presence of wild-type Axin1 constructs (Fig. 3C). This suggests that the Axin construct incorporating the *mbl* amino-acid change can interfere with wild-type Axin1 function in vitro. Despite this, embryos heterozygous for the *mbl* mutation have no obvious phenotype indicating that a single *mbl* allele does not lead to significant disruption of the function of wild-type Axin1 or related proteins in vivo. To test if high levels of the *mbl* allele of Axin1 could function in a dominant negative manner in vivo, we injected high concentrations of both wild-type and *mbl axin1*. Unfortunately, this led to the disruption of several processes (dorsoventral patterning, cell movements, and AP patterning) during gastrulation making interpretation of phenotypes problematic. These experiments did not allow us to unequivocally determine if the *mbl* allele of Axin1 does indeed have weak dominant-negative activity in vivo.

Excess Gsk3β can partially rescue the mbl *phenotype*

Association with Axin is believed to enable Gsk3 to efficiently phosphorylate β-catenin (Ikeda et al. 1998;Kishida et al. 1999), and so compromised Gsk3 activity in *mbl*$^{-/-}$ embryos may contribute to the *mbl*$^{-/-}$ phenotype. Indeed, wild-type zebrafish embryos treated with lithium, an inhibitor of Gsk3 (Klein and Melton 1996), have *mbl*-like phenotypes in which telencephalon and eyes are reduced or absent and trigeminal neurons are ectopically expanded (Macdonald et al. 1994). To test if reduced Gsk3 activity in *mbl*$^{-/-}$ mutants can be overcome by an excess of Gsk3, we overexpressed *gsk3*β RNA (Tsai et al. 2000) in *mbl*$^{-/-}$ embryos. About 30% of *mbl*$^{-/-}$ embryos overexpressing *gsk3*β had small eyes and this was also reflected by restoration of neural-plate patterning at earlier stages (Fig. 4A–F, Table 1). This data suggests that increasing Gsk3β activity can partially alleviate the requirement for Axin1 and supports the hypothesis that reduced Gsk3 activity contributes to the *mbl*$^{-/-}$ phenotype. It also indicates that Gsk3β still can have activity in the absence of wild-type Axin1, possibly through association with other Axin family proteins.

The mbl *mutation has no major consequences upon organizer/germ-ring formation or fates*

Taken together, the experiments described above suggest that compromised Axin1 function in *mbl*$^{-/-}$ embryos results in reduced Gsk3 activity with the consequence that less β–catenin is targeted for degradation and Wnt pathway target genes are overactivated. Activation of the Wnt pathway promotes organizer fates (Larabell et al. 1997) and the zebrafish organizer can indirectly influence anterior neural fates (Fekany et al. 1999;Saude et al. 2000;Shimizu et al. 2000;Sirotkin et al. 2000). This raises the possibility that the CNS phenotype of *mbl*$^{-/-}$embryos may be due to incorrect organizer function. However, unlike mutations such as *bozozok* (Koos and Ho 1999; Fekany-Lee et al. 1999, 2000) and *squint* (Feldman et al. 1998), which primarily affect organizer tissues, we observed apparently normal expression of *gsc*, *flh*, and other markers of organizer-derived mesendodermal fates in *mbl*$^{-/-}$ embryos (Fig. 1H; data not shown). This suggests that there is no major disruption to organizer function or fates in *mbl*$^{-/-}$ embryos.

Wnt8 is a candidate posteriorizing factor that can inhibit anterior neural fates and in *bozozok* and *tcf3/hdl* mutant embryos that lack forebrain structures, there is increased and ectopic expression of *wnt8* in germ-ring cells during gastrulation (Fekany-Lee et al. 2000;Kim et al. 2000). However, in clutches of embryos from heterozygous *mbl*$^{-/-}$ fish, we were unable to detect any obvious differences in *wnt8* expression between *mbl*$^{-/-}$ embryos and their siblings (data not shown). Therefore, *mbl*$^{-/-}$embryos do not show the same early alterations in gene expression that occur in embryos carrying other mutations that are known to directly or indirectly affect Wnt signaling activity.

Axin1/Mbl function is required during gastrulation for forebrain patterning

The apparent absence of major early patterning defects in *mbl*$^{-/-}$ embryos suggests that the *mbl* mutation may affect primarily Wnt-dependent patterning events after the onset of gastrulation. To address when Mbl/Axin1 may be required, we performed two sets of experiments. First, we transplanted wild-type ectodermal cells (taken from random positions in donor embryos) overexpressing *axin1* into the anterior neural plate of *mbl*$^{-/-}$ mutants at 70% epiboly stage. *axin1* expressing wild-type cells within the anterior neural plate partially rescue the *mbl*$^{-/-}$ mutant phenotype as determined by the expression of *fkd3* at bud stage and the presence of eyes at later stages (n = 9) (Fig. 4G–I; data not shown). Therefore, restoration of Axin1 function to neural plate cells during gastrulation is sufficient to restore anterior forebrain character in *mbl*$^{-/-}$ embryos. As a second approach, we made use of the temperature-dependent expressivity of the *mbl*$^{-/-}$ phenotype. To assess when Mbl function is required to promote eye development, we shifted *mbl*$^{-/-}$embryos from 28°C to 22°C at the onset and at the end of gastrulation. Five percent of embryos shifted to the lower temperature at the onset of

gastrulation had small eyes whereas embryos shifted at bud stage lacked eyes (Table 2). Together these studies suggest that suppression of Wnt activity during gastrulation stages influences the regional subdivision of the neural plate into telencephalic, diencephalic, and optic territories.

Axin1 also functions in early dorsoventral patterning

Mice lacking Axin function have multiple axes (Zeng et al. 1997) whereas *mbl*$^{-/-}$ fish embryos exhibit normal early dorsoventral patterning of mesodermal structures. This difference could be from the presence of maternally provided wild-type Axin1 in *mbl*$^{-/-}$ embryos. To assess if this may be the case, we injected antisense morpholino oligonucleotides (Nasevicius and Ekker 2000) against *axin1* into wild-type embryos ($n > 200$) and assessed effects upon the development of axial structures, using the organizer/notochord marker, *flh* (Fig. 4J). About 20% of injected embryos exhibited either marked dorsal expansion of the domain of *flh* expression (Fig. 4K) or ectopic expression of *flh* around the germ ring (Fig. 4L). About 50% of surviving injected embryos showed expansion of axial tissue at bud stage (data not shown). To confirm that the morpholino injections led to a reduction in Axin1 function, we performed Western blot analysis on wild-type and *axin1*-morpholino injected embryos. Weak anti-Axin immunoreactivity was detected in extracts of morpholino-injected embryos but levels were considerably reduced compared to wild-type (data not shown). We also confirmed phenotypes with two other *axin* morpholinos (data not shown). These results indicate that morpholino-based reduction in Axin1 function at early developmental stages can lead to the expansion, or ectopic induction, of axial structures. Therefore, it is likely that the function of Axin is conserved between mouse and fish, but that the *mbl* allele reveals a novel requirement for the gene that has not been amenable to study in mouse because of the severity of the early phenotype.

Wnt signaling establishes regional fates along the anterior-posterior axis of the prospective brain

Our study reveals a novel role for Axin1 in the regional subdivision of prospective forebrain territories. We propose that Wnt signaling must be suppressed to allow the development of telencephalic and optic fates and that if this fails to occur, prospective forebrain cells adopt a more caudal, diencephalic identity. It is intriguing that *headless/tcf3* mutant zebrafish embryos, in which the canonical Wnt pathway is also likely to be overactivated, show expansion of midbrain (or midbrain/hindbrain boundary) fates at the expense of forebrain fates (Kim et al. 2000). Similarly, graded overexpression of Wnt8 can lead to expansion of midbrain-specific gene expression into prospective forebrain territories (Fig. 4M–O). These observations raise the possibility that thresholds of Wnt activity may specify different posterior to anterior fates within the neural plate in a manner analogous to that proposed for graded Bmp activity in the allocation of fates along the dorsoventral axis of the neural plate (Barth et al. 1999;Nguyen et al. 2000).

Materials and methods

In-situ hybridization and antibody labeling

Antibody staining and in-situ hybridization with digoxygenin-incorporated antisense RNA probes was done as described (Heisenberg et al. 1996). Fish embryo raising and staging was done as described (Westerfield 1995).

Linkage analysis, mapping, and cloning

mbl^{tm213} was mapped in F2 offspring of a TÜ × WIK reference cross as described (Rauch et al. 1997), using Simple Sequence Length Polymorphism markers (Knapik et al. 1996) on pools

of 48 mutants and 48 siblings. Linkages from the pools were confirmed and refined by genotyping single embryos. To identify mutations, RNA from Tue wild-type and homozygous *mbl*^{tm213} embryos at bud stage was reverse-transcribed and then amplified by PCR with pfu polymerase for sequence analysis.

RNA and morpholino oligonucleotide injections

The wild-type *axin1* injection construct (pCS2SN*axin1*) was obtained from Dr. Hibi, Osaka University, and the wild-type *wnt8* injection construct from D r. R. Moon, Washington University. The mutated *mbl axin1* injection construct was assembled from two PCR fragments for which internal oligonucleotide primers were designed to introduce the $L^{399}\rightarrow Q$ amino-acid exchange using the wild-type pCS2SN*axin1* injection construct as template and subsequently cloned into the pCS2SN vector. RNA was injected into one-cell-stage embryos as described previously (Barth and Wilson 1995). Antisense *axin1 morpholino* oligonucleotides (sequences available on request) were injected at the one-cell stage or into individual blastomeres at early blastula stages. Injection of 2.5 ng *morpholino* antisense oligonucleotides/embryo led to reproducible phenotypes in the injected embryos. Results were comparable for both classes of injection and results shown in the paper are from injections at the one-cell stage. Western blot analysis (data not shown) used an affinity purified anti-Axin1 polyclonal antibody that revealed a band of expected size. Control *morpholino* oligonucleotides (Gene Tools) and *morpholino* antisense oligonucleotides against various other genes (*lfng*, *sqt*, *cyc*) were injected to determine the specificity of the obtained phenotypes. After phenotypic evaluation, in some cases, single embryos were genotyped taking advantage of a *Bpm*I restriction polymorphism induced by the *axin1/mbl* point mutation. Genomic DNA from single embryos was amplified a round the mutation site and the amplified fragment subsequently digested using *Bpm*I restriction enzyme.

Immunoprecipitation

Full-length murine Axin constructs were subcloned from a Myc-tagged Axin Form 1 cDNA (supplied by F. Constantini) into the CMV expression vector pcDNA3.1+ (Invitrogen). The N-terminal deletion construct was created using restriction enzymes (Smalley et al. 1999). The ΔNAxin L–Q mutation was created using the QuickChange Site-directed Mutagenesis Kit (Stratagene). The HA-tagged GSK-3β was made from pTM3β-tag (supplied by J. Woodgett) and cloned into pcDNA3.1+. 293 cells were transfected using FuGENE 6 (Boehringer Mannheim) according to the manufacturer's instructions and lysed 48 h later with a buffer containing 10mM Tris pH 7.5, 1 mM EDTA, NaCl 50 mM, 0.6 mM PMSF (Sigma Cat. No. P-7626), protease inhibitor cocktail (Sigma Cat. No. P8340), and 100 nM Okadaic Acid (Sigma Cat. No. O-1506). The cell lysates were precleared with 50 μL protein G sepharose beads (Amersham Pharmacia Biotech), previously washed in lysis buffer, for 30 min on a rotating wheel at 4°C. Aliquots containing 750 μg protein were made up to a volume of 500 μL and incubated, again on the rotating wheel at 4°C, with 2 μg antibody and 50 μL protein G sepharose beads for 4 h. The beads then were pelleted and washed three times with lysis buffer and used for Western analysis. Antibodies used were mouse α-Flag M 2 monoclonal antibody (Sigma), mouse α-HA monoclonal antibody 12CA5, and mouse α-GSK-3β (Transducin Labs).

Luciferase essay

293 cells were seeded at 7.5×10^4 cells/well in 6-well dishes (NUNC), 4 8 h before an experiment. Each well was transfected with 0.5 μg of one of the luciferase reporters TOPFLASH or FOPFLASH (Korinek et al. 1997), 0.15 μg of CMV-hTCF4 (Korinek et al. 1997), 2 5 ng of CMV-lacZ as an internal control and 0.3 ng of the test-construct (CMV-driven Flg-tagged ΔNAxin1). The CMV promoter-containing plasmid pcDNA3.1+ (Invitrogen) was used to equalize the total amount of CMV-driven plasmid per well. Carrier DNA (salmon

sperm) was added to a total of 2 μg. Transfection was done in triplicate using FuGENE 6 (Boehringer Mannheim) according to the manufacturers instructions. Luciferase and β-galactosidase activity were measured 48 h later. For the luciferase assays, cells were harvested into PBS and pelleted with a low-speed spin. Cell pellets then were lysed with reporter lysis buffer and processed to generate cell supernatant and pellet fractions according to manufacturer's recommendations (Promega Luciferase Assay system). Both fractions were kept for Western analysis. Luciferase activity in 20 μL supernatant fraction was measured in an AutoLumat LB953 (Berthold). For the β-galactosidase activity measurements, 20 μL of the supernatant fractions were used in a spectrometric kinetic assay based on the substrate CPRG (Boehringer Mannheim). Luciferase results were calculated after correcting for β-galactosidase activity. For Western analysis, the triplicate samples containing TOPFLASH were combined and the supernatant and pellets run separately on SDS-PAGE gels after normalizing protein loading for β-galactosidase expression. Unless otherwise stated, only data from supernatant fractions are presented adjacent to the luciferase TCF-transcription assay data. Antibodies used were mouse α-GSK-3β antibody (Transducin Labs) and mouse α-Flag M 2 monoclonal antibody (Sigma). Secondary antibodies used were against the appropriate species and HRP conjugated for visualization with enhanced chemiluminescence Western Blotting detection reagents (Amersham Pharmacia Biotech). Immunoblots shown in the figures are of the supernatant fraction unless otherwise stated.

Cell transplantations

Cell transplantations between wild-type and *mbl*$^{-/-}$ mutant embryos at midgastrulation stages were performed as previously described (Houart et a l. 1998).

Acknowledgements

We thank many colleagues who provided reagents that enabled us to test *axin1* and several other genes as candidates for the *mbl* mutation. In particular, we are indebted to Masahiko Hibi, Ken Irvine, Antonio Jacinto, Yun-Jin Jiang, Julian Lewis, and Tom Vogt for help and advice. We thank Ajay Chitnis and Dana Zivkovic for providing information prior to publication. This study was supported primarily by grants from the EMBO and EC to C.P.H., Wellcome Trust and EC to S.W.W., from the MRC to D.S., from Naito to M.T., from the DHGP to G.J.R. and R.G., and from the CRC/ICR to T.D. P.C. was supported by a PhD studentship from Fundação para a Ciência e Tecnologia, Programa PRAXIS XXI. S.W.W. is a Wellcome Trust Senior Research Fellow.

References

Aberle H, Bauer A, Stappert J, Kispert A, Kemler R. Beta-catenin is a target for the ubiquitin-proteasome pathway. EMBO J 1997;16:3797–3804. [PubMed: 9233789]

Barker N, Clevers H. Catenins, Wnt signaling and cancer. Bioessays 2000;22:961–965. [PubMed: 11056471]

Barth KA, Wilson SW. Expression of zebrafish nk2.2 is influenced by sonic hedgehog/vertebrate hedgehog-1 and demarcates a zone of neuronal differentiation in the embryonic forebrain. Development 1995;121:1755–1768. [PubMed: 7600991]

Barth KA, Kishimoto Y, Rohr KB, Seydler C, Schulte-Merker S, Wilson SW. Bmp activity establishes a gradient of positional information throughout the entire neural plate. Development 1999;126:4977–4987. [PubMed: 10529416]

Brown JD, Moon RT. Wnt signaling: Why is everything so negative? Curr Opin Cell Biol 1998;10:182–187. [PubMed: 9561842]

Fekany K, Yamanaka Y, Leung T, Sirotkin HI, Topczewski J, Gates MA, Hibi M, Renucci A, Stemple D, Radbill A, et al. The zebrafish bozozok locus encodes Dharma, a homeodomain protein essential for induction of gastrula organizer and dorsoanterior embryonic structures. Development 1999;126:1427–1438. [PubMed: 10068636]

Fekany-Lee K, Gonzalez E, Miller-Bertoglio V, Solnica-Krezel L. The homeobox gene bozozok promotes anterior neuroectoderm formation in zebrafish through negative regulation of BMP2/4 and Wnt pathways. Development 2000;127:2333–2345. [PubMed: 10804176]

Feldman B, Gates MA, Egan ES, Dougan ST, Rennebeck G, Sirotkin HI, Schier AF, Talbot WS. Zebrafish organizer development and germ-layer formation require nodal-related signals. Nature 1998;395:181–185. [PubMed: 9744277]

Gamse J, Sive H. Vertebrate anteroposterior patterning: The *Xenopus* neurectoderm as a paradigm. Bioessays 2000;22:976–986. [PubMed: 11056474]

Heisenberg CP, Brand M, Jiang YJ, Warga RM, Beuchle D, van Eeden FJ, Furutani-Seiki M, Granato M, Haffter P, Hammerschmidt M, et al. Genes involved in fore-brain development in the zebrafish, *Danio rerio*. Development 1996;123:191–203. [PubMed: 9007240]

Houart C, Westerfield M, Wilson SW. A small population of anterior cells patterns the forebrain during zebrafish gastrulation. Nature 1998;391:788–792. [PubMed: 9486648]

Ikeda S, Kishida S, Yamamoto H, Murai H, Koyama S, Kikuchi A. Axin, a negative regulator of the Wnt signaling pathway, forms a complex with GSK-3beta and beta-catenin and promotes GSK-3beta-dependent phosphorylation of beta-catenin. EMBO J 1998;17:1371–1384. [PubMed: 9482734]

Jacobs-Cohen RJ, Spiegelman M, Cookingham JC, Bennett D. Knobbly, a new dominant mutation in the mouse that affects embryonic ectoderm organization. Genet Res 1984;43:43–50. [PubMed: 6547105]

Jessell TM. Neuronal specification in the spinal cord: Inductive signals and transcriptional codes. Nat Rev Genet 2000;1:20–29. [PubMed: 11262869]

Kim CH, Oda T, Itoh M, Jiang D, Artinger KB, Chandrasekharappa SC, Driever W, Chitnis AB. Repressor activity of Headless/Tcf3 is essential for vertebrate head formation. Nature 2000;407:913–916. [PubMed: 11057671]

Kim L, Liu J, Kimmel AR. The novel tyrosine kinase ZAK1 activates GSK3 to direct cell fate specification. Cell 1999;99:399–408. [PubMed: 10571182]

Kishida S, Yamamoto H, Hino S, Ikeda S, Kishida M, Kikuchi A. DIX domains of Dvl and axin a re necessary for protein interactions and their ability to regulate beta-catenin stability. Mol Cell Biol 1999;19:4414–4422. [PubMed: 10330181]

Klein PS, Melton DA. A molecular mechanism for the effect of lithium on development. Proc Natl Acad Sci 1996;93:8455–8459. [PubMed: 8710892]

Knapik EW, Goodman A, Atkinson OS, Roberts CT, Shiozawa M, Sim CU, Weksler-Zangen S, Trolliet MR, Futrell C, Innes BA, et al. A reference cross DNA panel for zebrafish (*Danio rerio*) anchored with simple sequence length polymorphisms. Development 1996;123:451–460. [PubMed: 9007262]

Koos DS, Ho RK. The nieuwkoid/dharma homeobox gene is essential for bmp2b repression in the zebrafish pregastrula. Dev Biol 1999;215:190–207. [PubMed: 10545230]

Korinek V, Barker N, Morin PJ, van Wichen D, de Weger R, Kinzler KW, Vogelstein B, Clevers H. Constitutive transcriptional activation by a beta-catenin-Tcf complex in $APC^{-/-}$ colon carcinoma. Science 1997;275:1784–1787. [PubMed: 9065401]

Larabell CA, Torres M, Rowning BA, Yost C, Miller JR, Wu M, Kimelman D, Moon RT. Establishment of the dorsoventral axis in *Xenopus* embryos is presaged by early asymmetries in beta-catenin that are modulated by the Wnt signaling pathway. J Cell Biol 1997;136:1123–1136. [PubMed: 9060476]

Lee KJ, Jessell TM. The specification of dorsal cell fates in the vertebrate central nervous system. Annu Rev Neurosci 1999;22:261–294. [PubMed: 10202540]

Lumsden A, Krumlauf R. Patterning the vertebrate neuraxis. Science 1996;274:1109–1115. [PubMed: 8895453]

Macdonald R, Xu Q, Barth KA, Mikkola I, Holder N, Fjose A, Krauss S, Wilson SW. Regulatory gene expression boundaries demarcate sites of neuronal differentiation in the embryonic zebrafish forebrain. Neuron 1994;13:1039–1053. [PubMed: 7946344]

Masai I, Heisenberg CP, Barth KA, Macdonald R, Adamek S, Wilson SW. Floating head and masterblind regulate neuronal patterning in the roof of the fore-brain. Neuron 1997;18:43–57. [PubMed: 9010204]

Nasevicius A, Ekker SC. Effective targeted gene 'knockdown' in zebrafish. Nat Genet 2000;26:216–220. [PubMed: 11017081]

Nguyen VH, T rout J, Connors SA, Andermann P, Weinberg E, Mullins MC. Dorsal and intermediate neuronal cell types of the spinal cord are established by a BMP signaling pathway. Development 2000;127:1209–1220. [PubMed: 10683174]

Niehrs C. Head in the WNT: The molecular nature of Spemann's head organizer. Trends Genet 1999;15:314–319. [PubMed: 10431193]

Rauch, G.-J., Granato, M., and Haffter, P. 1997. A polymorphic zebrafishline for genetic mapping using SSLPs on high-percentage agarose gels. Technical Tips Online T01208.

Saude L, Woolley K, Martin P, Driever W, Stemple DL. Axis-inducing activities and cell fates of the zebrafish organizer. Development 2000;127:3407–3417. [PubMed: 10903167]

Shimizu T, Yamanaka Y, Ryu SL, Hashimoto H, Yabe T, Hirata T, Bae YK, Hibi M, Hirano T. Cooperative roles of Bozozok/Dharma and Nodal-related proteins in the formation of the dorsal organizer in zebrafish. Mech Dev 2000;91:293–303. [PubMed: 10704853]

Sirotkin HI, Dougan ST, Schier AF, Talbot WS. bozozok and squint act in parallel to specify dorsal mesoderm and anterior neuroectoderm in zebrafish. Development 2000;127:2583–2592. [PubMed: 10821757]

Smalley MJ, Sara E, Paterson H, Naylor S, Cook D, Jayatilake H, F ryer LG, Hutchinson L, Fry MJ, Dale TC. Interaction of axin and Dvl-2 proteins regulates Dvl-2-stimulated TCF-dependent transcription. EMBO J 1999;18:2823–2835. [PubMed: 10329628]

Tsai JN, Lee CH, Jeng H, Chi WK, Chang WC. Differential expression of glycogen synthase kinase 3 genes during zebrafish embryogenesis. Mech Dev 2000;91:387–391. [PubMed: 10704871]

Webster MT, Rozycka M, Sara E, Davis E, Smalley M, Young N, D ale TC, Wooster R. Sequence variants of the axin gene in breast, colon, and other cancers: An analysis of mutations that interfere with GSK3 binding. Genes Chromosomes Cancer 2000;28:443–453. [PubMed: 10862053]

Westerfield, M. 1995. *The Zebrafish Book* University of Oregon Press, Salem, OR.

Wilson SW, Rubenstein JL. Induction and dorsoventral patterning of the telencephalon. Neuron 2000;28:641–651. [PubMed: 11163256]

Wodarz A, Nusse R. Mechanisms of Wnt signaling in development. Annu Rev Cell Dev Biol 1998;14:59–88. [PubMed: 9891778]

Zeng L, Fagotto F, Zhang T, Hsu W, Vasicek TJ, Perry WL 3rd, Lee JJ, Tilghman SM, Gumbiner BM, Costantini F. The mouse Fused locus encodes Axin, an inhibitor of the Wnt signaling pathway that regulates embryonic axis formation. Cell 1997;90:181–192. [PubMed: 9230313]

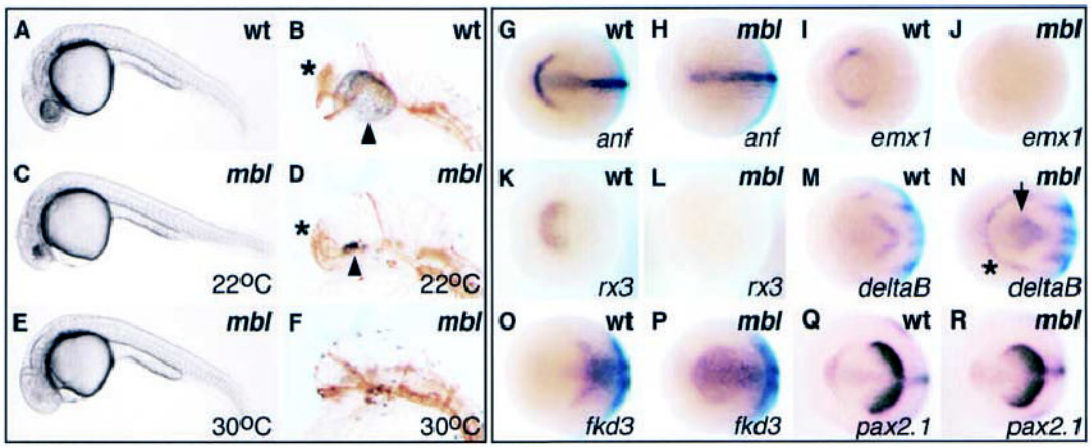

Figure 1.

mbl$^{-/-}$ embryos exhibit fate transformations within the forebrain. (*A*,*C*,*E*) Lateral views of living wild-type (*A*) and *mbl*$^{-/-}$embryos raised at 22°C (*C*) and 30°C (*E*). (*B*,*D*,*F*) Lateral views of forebrains of wild-type (*B*) and *mbl*$^{-/-}$ embryos raised at 22°C (*D*) and 30°C (*F*) stained with an α-acetylated tubulin antibody. Eyes (arrowheads) and telencephalon (asterisks) are reduced in the embryo raised at 22°C, whereas they are absent in the embryo raised at 30°C indicating that the *mbl* mutation is temperature-sensitive. (*G–R*) Differences in gene expression between neural plates of *mbl*$^{-/-}$ (*mbl*) and wild-type embryos. Genes analyzed a re indicated at *bottom right*. Axial mesendodermal tissue is labeled additionally with a *flh* probe in (*G*,*H*) and *gsc* and *flh* probes in (*Q*,*R*). For *deltaB* (*M*,*N*), both diencephalic expression (arrow) and expression in prospective trigeminal neurons (asterisk) is rostrally expanded in the *mbl*$^{-/-}$embryo. Gene expression characteristic of telencephalic and eye field fates (*G–L*) are reduced or absent in *mbl*$^{-/-}$ embryos while gene expression characteristic of more caudal diencephalic fates (*M–P*) is expanded.

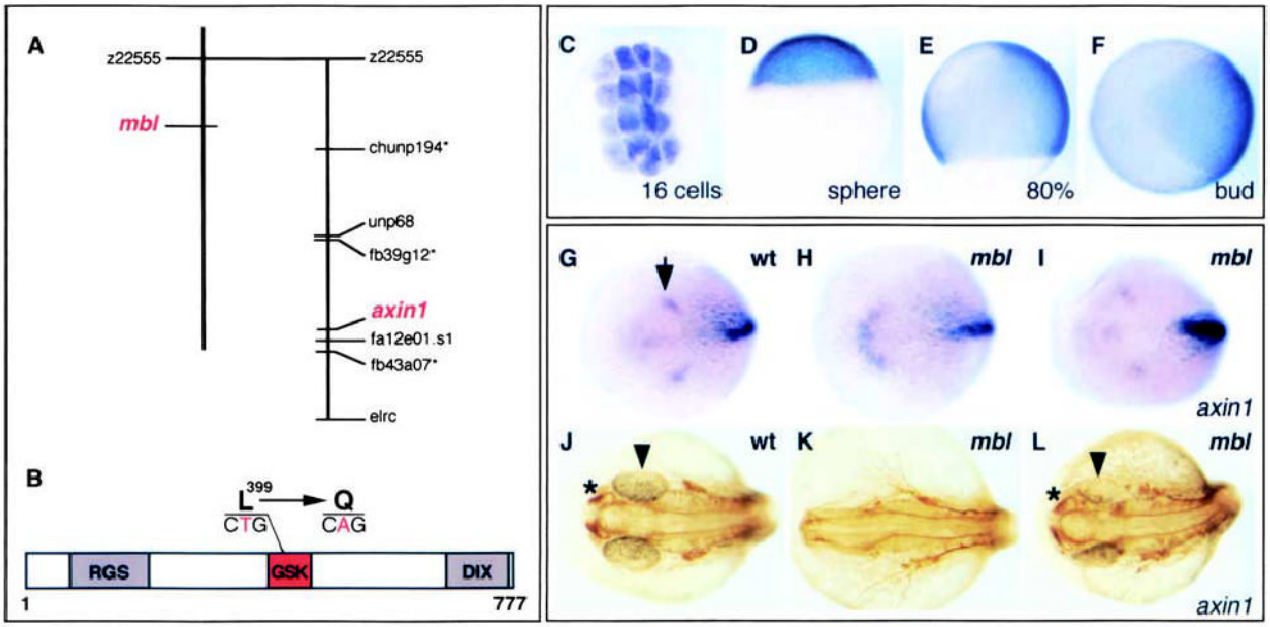

Figure 2.

mbl$^{-/-}$ embryos harbor a mutation in the *axin1* gene. (*A*) Mapping of *mbl* on linkage group 3 close to *axin1* on the corresponding region of a radiation hybrid map. (*B*) Schematic representation of the Axin1 protein showing the amino-acid exchange (L^{399}→Q) and underlying point mutation (T→A) within the predicted Gsk3 binding site in the *mbl* Axin1 allele. (*C–F*) Localization of *axin1* transcripts in lateral (*D,E*) and animal pole (*C,F*) views of wild-type embryos at the 1 6 cell stage (*C*), sphere stage (*D*), 80% epiboly (*E*) and bud stage (*F*). *axin1* transcripts are maternally provided and ubiquitously expressed in wild-type embryos. (*G–L*) Phenotypes of wild-type (*G,J*), *mbl*$^{-/-}$ (*H,K*), and *mbl*$^{-/-}$ embryos injected with *axin1* RNA (*I,L*) stained for the expression of *flh* in the epiphysial region of the diencephalon (arrow,*G*) at bud stage (*G–I*) or stained with α-acetylated tubulin antibody at pharyngula stage (*J–L*). Injection of *axin1* RNA at the one-cell-stage rescues the *mbl*$^{-/-}$ mutant phenotype determined by the pattern of *flh* expression at bud stage and the presence of telencephalon (asterisks) and eyes (arrowheads) at pharyngula stage.

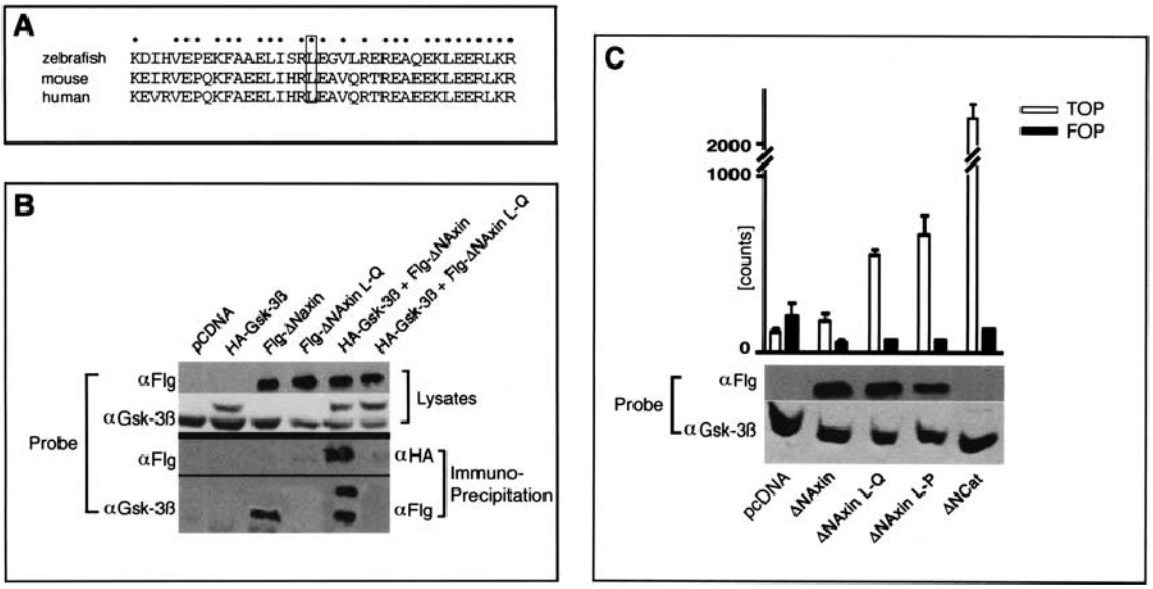

Figure 3.

The *mbl* mutation a bolishes binding of Axin to Gsk3. (*A*) Comparison of the amino-acid sequence around the L→Q mutation site within the Gsk3 binding domain of Mbl/Axin1 between zebrafish, mouse, and human shows a high degree of conservation. (*B*) Assessment of binding of Gsk3 β to a wild-type Axin construct (FlgΔN-Axin) and to an Axin construct incorporating the L→Q amino-acid exchange (FlgΔN-Axin L–Q). Wild-type and/or mutant (L–Q) FlgΔN-Axin and HA-Gsk3β were immunoprecipitated and immunoblotted with α-Gsk-3β and α-Flg antibodies. The L–Q mutation prevents both endogenous Gsk-3-β and HA-Gsk-3β association with the Axin protein. The ΔN variant of Axin (amino acids 351–965) was used in preference to full length Axin because of its greater solubility in vitro (Smalley et al. 1999). (*C*) Assessment of TCF-dependent transcription in the presence of Flg-ΔNAxin and Flg-ΔNAxin L–Q. Expression of Flg-ΔNAxin L–Q activates TCF-dependent transcription indicating that it can act as a dominant active protein while wild-type Flg-ΔNAxin has little or no effect compared to control (pcDNA). The dominant effect of Flg-ΔNAxin L–Q is comparable to the previously described L–P mutation at the same position (lane*4;* Smalley et al. 1999). Expression of transfected Axin and endogenous Gsk3β (control) is shown by immunoblot analysis. Lane *5* shows transcription following transfection with a constitutively active form of beta;-catenin. Counts are luciferase reporter assay readouts from TOP-FLASH plasmid (TCF-binding motif) and FOP-FLASH plasmid (mutant motif as control) that have been adjusted for transfection efficiency as described previously (Smalley et al. 1999).

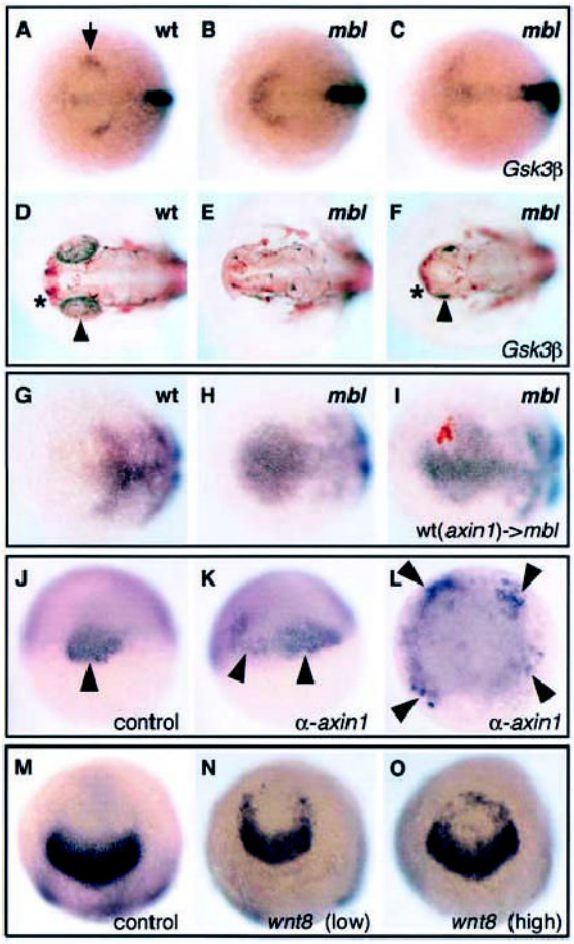

Figure 4.

Mbl/Axin1 functions both in anterior neural plate patterning and axis development. (*A–F*) Dorsal views of neural plates and brains of wild-type (*A,D*), *mbl*$^{-/-}$ (*B,E*), and *mbl*$^{-/-}$ embryos injected with *gsk3* β RNA (*C,F*) stained for the expression of *flh* in the epiphysial region of the diencephalon (arrow, *A*) at bud stage (*A–C*) or stained with an α-acetylated tubulin antibody at pharyngula stage (*D–F*). The embryos injected with *gsk3*β RNA show partial rescue of the*mbl*$^{-/-}$ phenotype as determined by the pattern of *flh* expression at bud stage and the presence of telencephalon (asterisk) and small eyes (arrowhead) at pharyngula stage. (*G–H*) Dorsal views of neural plates of wild-type (*G*), *mbl*$^{-/-}$ (*H*), and *mbl*$^{-/-}$ embryos in which wild-type cells expressing *axin1* RNA were transplanted into the anterior neural plate at 70% epiboly stage (*I*) showing expression of *fkd3* (characteristic of mid/caudal diencephalon identity in wild-type) at bud stage. Ectopic rostral *fkd3* expression is absent in the transplanted cells and in some of the *mbl*$^{-/-}$ host cells adjacent to the transplanted cells. (*J–L*) Dorsal (*J,K*) and animal pole (*L*) views of a wild-type embryo and embryos injected with α-*axin1* morpholino antisense oligonucleotides (*K,L*) stained for the expression of *flh* (a marker of organizer tissue, arrowheads) at shield stage. (*J*) An uninjected wild-type control embryo showing a single expression domain of *flh* within the dorsal organizer region. In (*K*), the injected embryo shows expansion of *flh* expression on the dorsal side of the embryo. In (*L*), the injected embryo has multiple sites of *flh* expression indicative of widespread dorsalization. (*M–O*) Animal pole views of bud-stage control embryo (*M*) or embryos injected with increasing (*left* to *right*) doses of *wnt8* RNA (*N,O*). In addition to variably causing dorsalization (data not shown), *pax2.1/noi* expression (normally restricted to the presumptive midbrain), spreads into the anteriormost

regions of the neural plate of injected embryos. This expansion is unlikely to be simply a result of dorsalization of the ectoderm, as inhibition of BMP signaling also dorsalizes ectoderm but does not lead to anterior expansion of *pax2.1* expression (e.g., Barth et al. 1999).

Table 1

Wild-type Axin1 rescues eye[1] *development in* mbl$^{-/-}$ *embryos*

Injected RNA	Genotype	Normal (n)	Absent (n)	Small (n)	Total (n)
GFP (control)	*mblxmbl*	78	27	0	105
axin1(L→Q)	*mblxmbl*	87	29	0	116
axin1	*mblxmbl*	77	0	20	97
*gsk3*β	*mblxmbl*	73	15	8	96

[1] Size of the eyes was scored at pharyngula stage. 1 0 pg/embryo of *GFP*, *axin1* and *axin1* (L→Q) RNA, and 200 pg/embryo of *gsk3*β RNA were injected.

Table 2

mbl *is a temperature-sensitive mutation affecting eye*[1] *development*

Temp (°C)	Genotype	Normal (n)	Absent (n)	Small (n)	Total (n)
28	*mblxmbl*	126	38	0	164
22	*mblxmbl*	118	32	13	163
28→22[2]	*mblxmbl*	148	42	11	201
28→22[3]	*mblxmbl*	155	48	0	203

[1] Size of the eyes was scored at pharyngula stage;

[2] embryos were shifted from 28°C to 22°C at shield stage;

[3] embryos were shifted from 28°C to 22°C at bud stage.